ISSN 1027-5495. Functional Materials, 29, No.2 (2022), p. 291-298.
doi:https://doi.org/10.15407/fm29.02.291

Development of technology for forming vacuum-arc TiN coatings using additional impulse action

N.V.Pinchuk, V.V.Starikov, H.O.Kniazieva, S.V.Surovytskyi, N.V.Konotopska

National Technical University "Kharkiv Polytechnic Institute",
2 Kyrpychova Str., 61002 Kharkiv, Ukraine

Received February 14, 2022

The effect of supplying a constant and high-voltage pulse with duration of 10 μs on the formation of predominantly oriented crystallites and the stress-strain state of vacuum-arc TiN coatings at two pressures of a nitrogen atmosphere is analyzed. It is shown that the deposition of the coatings under conditions of high voltage cascading effect leads to the growth of crystallites with the texture axis [110] and to a change in the stress-strain state (reduction of deformation in the group of crystallites with the axis [111]). The obtained results are explained by an increase in the mobility of atoms and ordering processes in the region of the displacement cascades formed under the action of bombarding high-energy ions accelerated in the field of high-wave pulse potential. Computer simulations of the main processes observed during deposition were performed.

Keywords: TiN, coating, pulse influence, computer simulation, duration, radiation factor, texture, deformation.

Розробка методики формування вакуумно-дугових покриттів TiN при додатковому імпульсному впливі. *Н.В.Пінчук, В.В.Старіков, Г.О.Князєва, С.В.Суровицький, Н.В.Конотопська*

Проаналізовано вплив подачі постійного та високовольтного імпульсного потенціалу тривалістю 10 мкс на формування переважно орієнтованих кристалітів та напружено-деформований стан вакуумно-дугових покриттів TiN при двох тисках азотної атмосфери. Показано, що нанесення покриттів в умовах високовольтної каскадної дії призводить до зростання кристалітів з віссю текстури [110] та зміни напружено-деформованого стану (зниження деформації в групі кристалітів з віссю текстури [111]). Отримані результати пояснюються збільшенням рухливості атомів і процесами впорядкування в області каскадів зміщення, що утворюються під дією високоенергетичних бомбардуючих іонів, прискорених в полі високовольтного імпульсного потенціалу. Проведено комп'ютерне моделювання основних процесів, що спостерігаються під час осадження.

1. Introduction

At the present stage of technical progress and the general trend towards a decrease in material consumption, it is extremely important to reduce the rigidity of structures, increase the carrying capacity and efficiency of machines, their reliability and durability. To solve this fundamental general technical problem, one of requirements is to ensure a high level of wear resistance and a period of trouble-free operation of parts and assemblies of military equipment. According to various estimates, from 60 % to 90 % of malfunctions and failures in the operation of machines and mechanisms occur due to deformation and wear [1, 2], and the associated destruction of parts.

The problem of combating these negative phenomena has been in the focus of attention of specialists in various fields of mechanical engineering for many years [3–8], but even now it remains not fully resolved. The complexity of the problem of protection against destruction of machine parts is largely due to insufficient understanding of wear mechanisms, the lack of criteria and methods for assessing and predicting the performance of tribosystems, taking into account various forms and conditions of interaction. Currently, much attention is paid to the production of submicron, nanocrystalline materials and the study of their properties in connection with their application in various fields of technology, such as electronics, catalysis, magnetic storage of information, structural elements, etc. [9–11]. Submicron and nanocrystalline metallic and ceramic materials are widely used as structural elements and functional layers in modern microelectronic devices, aerospace parts, as well as hard wear-resistant coatings [12–18].

2. Experimental

All samples were obtained using modern coating methods on a modernized "Bulat-6" installation, additionally equipped with a high-voltage potential generator in a pulsed mode [19]. The nitrogen pressure (pN_2) in the vacuum chamber during deposition was $2 \cdot 10^{-3}$ Torr and $5 \cdot 10^{-3}$ Torr. The value of the constant bias potential was $U_s = -230$ V, and the high-voltage pulse potential (U_i) was –600 V, –1200 V and –2000 V (with a frequency of 7 kHz and a duration of exposure of 10 μs). The duration of the deposition process ranged from 1 to 2 hours. Stainless steel plates $12Cr_{18}Ni_{10}Ti$ (analog of stainless steel SS 321) in the sizes 18×18×2 mm were used as substrates.

Structure of the samples was studied using a "DRON-3M" instrument in Cu–Kα radiation. A graphite monochromator was installed in the secondary beam (in front of the detector) [20]. The measurements were carried out in the 2θ angle range from 20° to 80°, containing all diffraction reflections from close-packed planes. Scanning step was $\Delta\theta = 0.1°$.

The substructural characteristics were analyzed by the method of approximating the shape of two orders of diffraction reflections from the planes of the crystal lattice using the Cauchy approximation function [21]. To study the stress-strain state, the method of multiple oblique recordings (a-$\sin^2$-method) and the method of crystal groups were used [22, 23]. Microindentation was performed on a "Micron-gamma" device [24, 25] at room temperature (load up to 0.5 N) with a Berkovich diamond pyramid.

Computer simulation of ion-plasma implantation was performed using the TRIM program in the "Monolayer Collision Steps/Surface Sputtering" mode [20]. In this simulation mode, all cascade damages are taken into account. Each atom is considered until its energy falls below the minimum threshold energy of displacement of any target atom. Thus, the target damages occurred during the collision are analyzed.

3. Results and discussion

1. Computer simulation

The simulations were performed for two cases — for the TiN system, which was subjected to nitrogen ion bombardment, and for the TiN system, which was subjected to titanium ion bombardment. For each of these two cases, different energies were chosen that most correspond to the real conditions for obtaining coatings from titanium nitride: 600, 1200, and 2000 eV. Six different cases were considered, in each of them the first ten iterations were considered, the most informative for comparison with real films; and cascades of thousands of iterations were considered to get an overall picture of the simulated processes. Tables 1 and 2 show the simulation results. Table 1 shows the depth of penetration of ions into the coating; Table 2 represents the number of vacancies that create ions during the bombardment. Due to the large number of results, the tables show the simulation results obtained at 1000 iterations.

Energy 600 eV. According to the simulation results of the first ten iterations for the potential of 600 V, the maximum penetration depth of nitrogen ions is approximately 4 nm, which is half the maximum penetration depth per thousand iterations, equal to 8 nm (Table 1). The largest accumulation of ions is observed at a depth of about 1.5–3 nm. The radius of the zone in which the coating is formed is approximately 4 nm. During the bombardment process, a large number of vacancies are created. Table 2 shows histograms of vacancies at thousands of iterations, from which it is possible to find out the number of vacancies formed by one ion at a certain depth of the layer; the maximum of the histogram coincides with the zone of the

Table 1. Ion penetration depth, 1000 iterations (simulation results)

U, V	Ion - coating	
	N-TiN	Ti-TiN
600	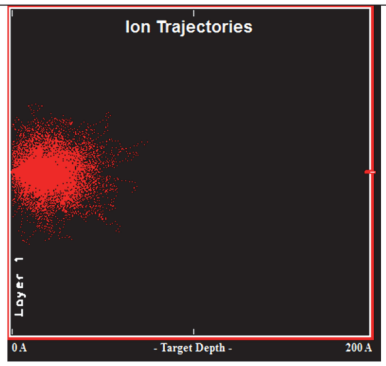	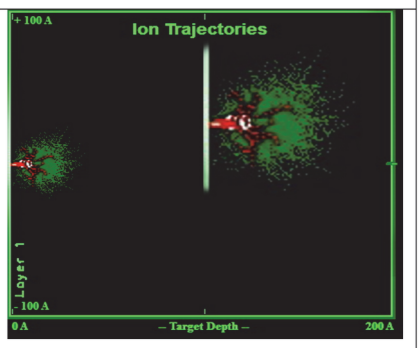
1600	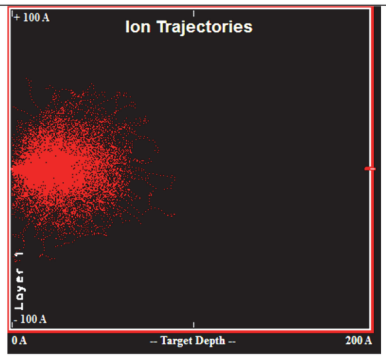	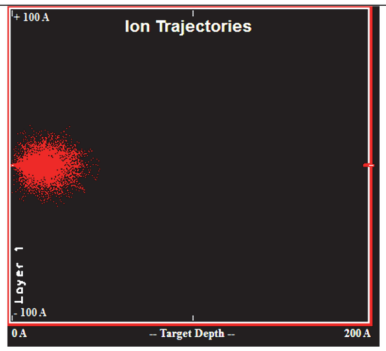
2000	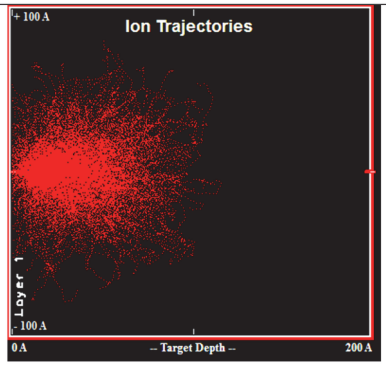	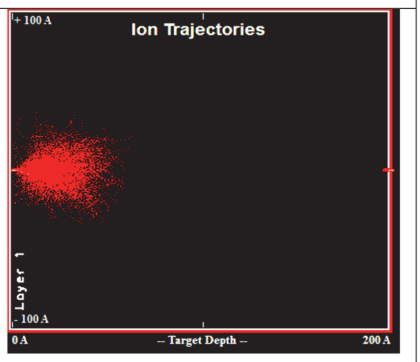

greatest accumulation of ions and is located at a depth of 1.2–1.5 nm. Table 1 shows the results of modeling the implantation of ten titanium ions against the background of thousands of ions falling into the coating. The further direction of the formation of the coating with an increase in the number of iterations can be seen along the trajectory of movement. As in the first case, the zone of the largest accumulation is at a depth of 1.5–3 nm, and the maximum depth of penetration of titanium ions into the substrate is 4 nm. The number of vacancies formed during the first iterations is a maximum of 1.4 vacancies per ion at a depth of 3 nm; with an increase in the number of iterations, this value gradually decreases, and for thousands of ions it is about 1 vacancy per ion at a depth of 1.5 nm (Table 2).

Energy 1200 eV. With an increase in the energy of nitrogen ions from 600 eV to 1200 eV, there is an increase in the depth of penetration from 8 nm to 9 nm; in addition, the region of the greatest accumulation of ions also increases and is located at a depth of 0.5–5 nm, and the center of this region is located at a depth of about 2 nm (Table 1). It should be added that with an

Table 2. Simulation results for the number of vacancies due to ion bombardment at 1000 iterations

U, V	Ion - coating	
	N-TiN	Ti-TiN
600	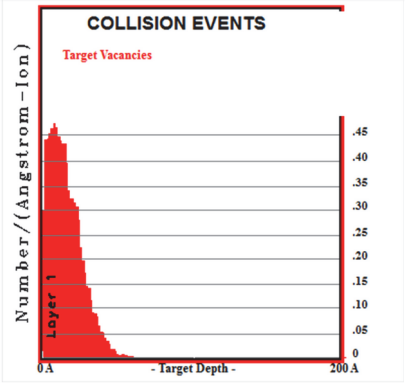	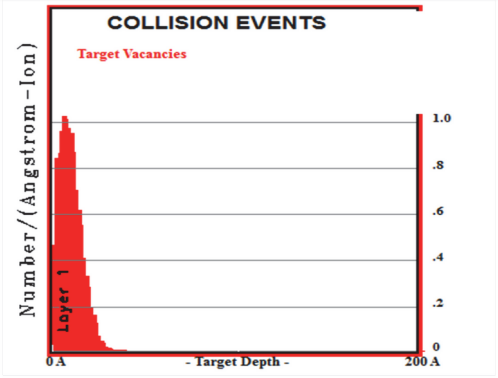
1200	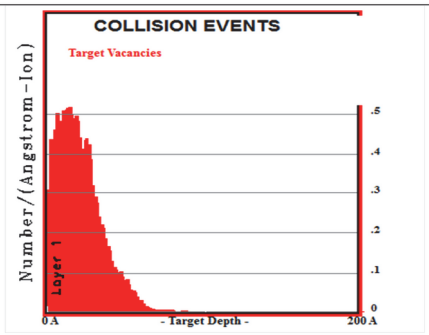	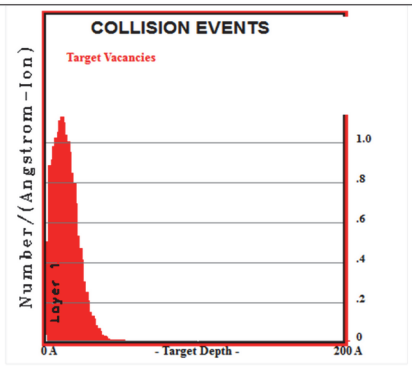
2000	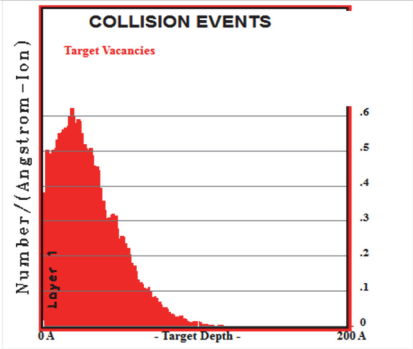	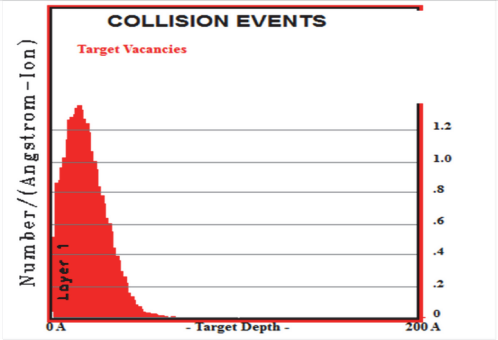

increase in the energy of nitrogen ions, the zone in which the coating is formed does not increase significantly and its radius is approximately 4–4.5 nm (Table 1). At the same depth, there is a maximum of the histogram of vacancies created by nitrogen ions (Table 2); with distance from the center of this zone, the number of vacancies formed by one ion decreases.

With increasing energy, there is a change in the trajectory of titanium ions, for example, in the first ten iterations, there are two directions in which the ions move. In this case, in contrast to the previous one, no significant increase in the penetration depth of titanium ions is observed; only an increase in the region of the largest accumulation of ions can be distinguished, which is located at a depth of 1 to 4 nm (Table 1). The location and number of vacancies formed by one titanium ion changed. Thus, at the first iterations, the number of vacancies per ion is about 2.5, and with further development of the process, this value decreases to 1.1 at a thousand iterations (Table 2).

Energy 2000 eV. With a further increase in energy to 2000 eV, there is an expansion

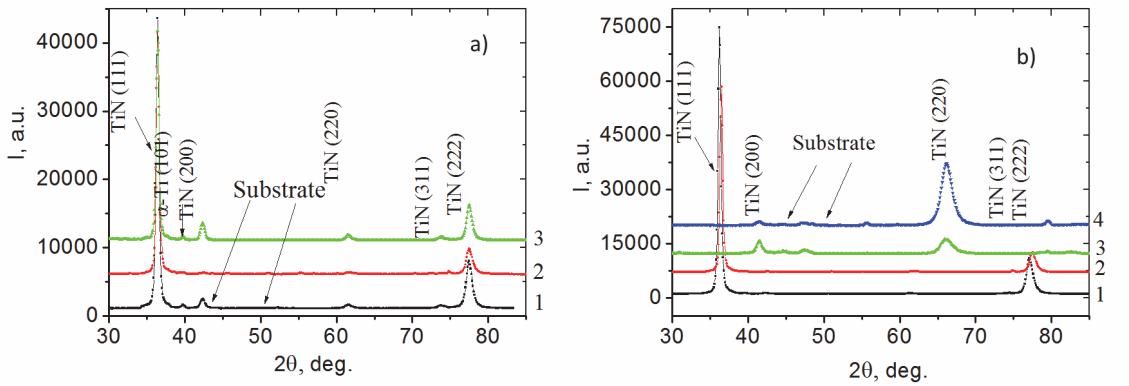

Fig. 1. XRD patterns of TiN coatings obtained at U_s = −230 V, p_N = 2·10^{-3} Torr (a), p_N = 5·10^{-3} Torr (b), τ = 10 μs: *1* — U_i = 0 V; *2* — U_i = −600 V; *3* — U_i= −1200 V; *4* — U_i = −2000 V.

of the region into which the ions fall, the zone of the greatest accumulation of ions has also expanded and this zone is located at a depth of 11.5–12 nm (Table 1).

The vacancy histogram also changed; if at a lower energy there was only one maximum, then at this energy there are several maxima at ten iterations, but with a larger number of ions the histogram flattens out and again one maximum remains (Table 2). With an increase in energy of the bombardment with titanium ions, there is an increase in the depth of penetration of ions, but the zone of the largest accumulation of ions remains unchanged, only the number of ions outside this zone increases (Table 1).

At impact energy of 2000 eV, the histogram of vacancies has the same appearance as in the previous case; for example, with ten iterations, the histogram can be divided into two parts, each of which has its own maximum, but with an increase in the number of iterations, the second maximum disappears, only one remains, located at a depth of 2 nm (Table 2). In addition, as in the previous cases, there is a decrease in the number of vacancies per ion from 1.9 at ten iterations to 1.3 at a thousand iterations.

Thus, for the cases described above, we can conclude that with increasing energy, the depth of penetration of ions increases; the distribution of vacancies along the depth of the layer changes in a certain way, which indicates a change in the processes occurring during the deposition of TiN coatings. The large difference in the depth of penetration between nitrogen and titanium ions is due to the size of the ions; since the size of titanium ions is much larger than nitrogen ones, they have less ability to penetrate deeper into the surface. To study the structure of the coating surface, it is important to simulate cascades with a small number of iterations, since large cascades form a loose zone through which ions can penetrate deep into the coating; that is, they will affect the structure and properties in the bulk of the material, but not in the near-surface regions.

2. X-ray structural studies of coatings

The diffraction spectra obtained from the coatings deposited at different values of the pulse negative bias potential, in the entire studied range of operating pressures p_N = (2·10^{-3}...5·10^{-3}) Torr, show reflections of only one nitride phase — TiN mononitride with a cubic crystal lattice of the NaCl structural type (JCPDS 38-1420) (Fig. 1a, b). An increase in the perfection of the texture with the [111] axis with increasing pressure can be noted as a characteristic tendency, which is clearly seen from an increase in the relative intensity of the peaks by two orders of magnitude from the (111) and (222) planes in the spectra presented. Fig. 1a shows the areas of diffraction spectra of TiN coatings obtained at the lowest pressure of the nitrogen atmosphere (p_N = 2·10^{-3} Torr; and Fig. 1b corresponds to p_N = 5·10^{-3} Torr. It was found that pulse action (0.6 kV) does not lead to violation of the trend to increase the degree of texturing of the coating (spectrum 2 in Fig. 1a, b).

The difference associated with the effect of pulsed stimulation is manifested in the change in the width of the diffraction reflections, which is determined by the difference in substructural characteristics. It should be noted that with increasing pulse displacement potential to 1200 V and 2000 V and the highest pressure of the nitrogen atmosphere (p_N = 5·10^{-3} Torr), a strong texture with an axis [110] parallel to the incident beam of high-energy film-forming particles is observed. Given the previous

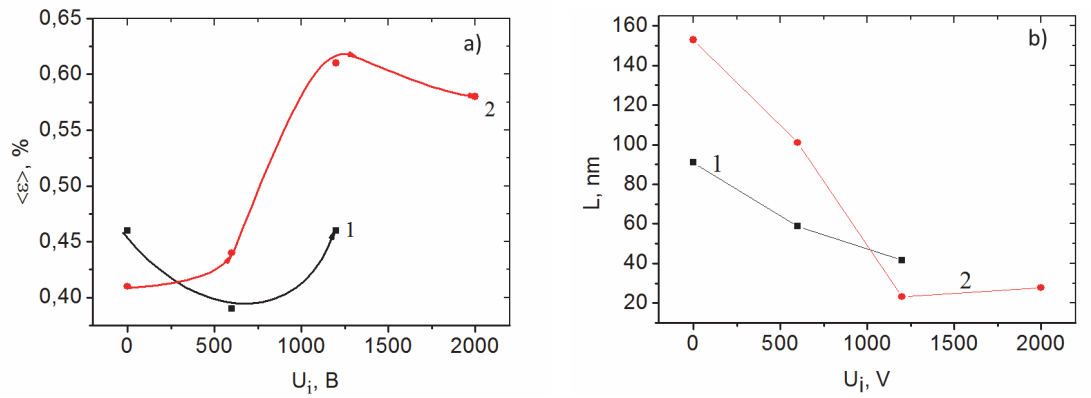

Fig. 2. Dependence of microstrain (a) and crystallite size (b) on the value of the pulsed bias potential for TiN coatings obtained at U_s = −230 V, τ = 10 μs and different pressures p_N: *1* — $2{\cdot}10^{-3}$ Torr; *2* — $5{\cdot}10^{-3}$ Torr.

results [26], the same tendency to form a strong texture [110] can be observed at a pressure of $p_N = 2{\cdot}10^{-3}$ Torr with increasing U_i. It should be noted that it is the complex action of pulsed and constant displacement potentials that has a significant effect on the growth texture in these coatings.

The next stage of the study was to determine the substructural characteristics using the method of approximation of the diffraction line shape by the Cauchy function. The results are presented in Fig. 2a, b.

From the graphs obtained, one can see a non-monotonic change in microstrains both under pulse action and in its absence. The lower value of microstrains at $p_N = 2{\cdot}10^{-3}$ Torr at a pulsed bias voltage of −600 V can be associated with ordering processes in the crystal lattice. With a further increase in the value of the pulsed bias voltage for two pressures, the microstrains increase; this is associated with a more intense accumulation of defects during the growth of the nitride coating under nonequilibrium deposition conditions. It should be noted that the level of microstrains is higher at a pressure of $p_N = 5{\cdot}10^{-3}$ Torr, than at $p_N = 2{\cdot}10^{-3}$ Torr, which is associated with an increase in the number of film-forming particles implanted in the coating surface. In this case, the relaxation processes do not have time to occur. Fig. 2b shows the dependence of crystallite size on the magnitude of the pulsed bias potential. With an increase of the magnitude of the pulsed bias potential, a decrease in the size of the crystallites is observed for both pressures. This indicates a more significant impact of implantation processes during deposition. That is, due to intense ion bombardment, defects accumulate, which contributes to grain refinement.

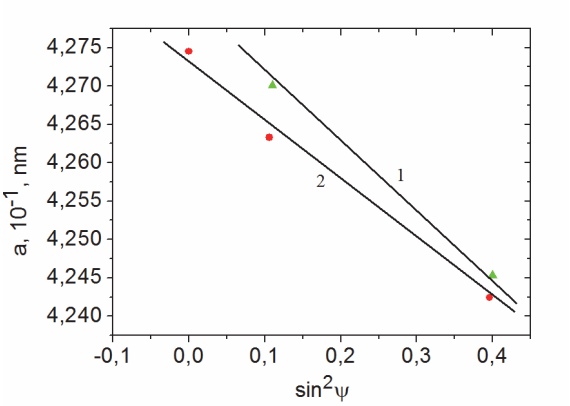

Fig. 3. Comparative "a – $\sin^2\psi$-graphs for TiN coatings obtained at $p_N = 5{\cdot}10^{-3}$ Torr and a constant bias potential of −230 V: *1* — without pulsed action, *2* — at U_i = −600 V

The appearance of a second predominant orientation of crystallite growth also contributes to a decrease in the crystallite size [26].

To evaluate the stress-strain state, the a-$\sin^2\psi$ method was used; in the case of a strong axial texture, its modification based on oblique measurements at different crystallographically given angles was applied. In addition to the reflections from the texture planes, the reflections from the planes (420), (422) and (511) at the angles corresponding to the texture planes were used. According to the results of such measurements for TiN coatings, a-$\sin^2\psi$ — graphs were constructed, the experimental points of which are well described by the linear dependence (Fig. 3). The slope of the graphs indicates the presence of high compressive macrostrains in the coatings. It is seen that with increasing constant bias potential on the substrate, the residual stress level and the crystal lattice period of titanium nitride

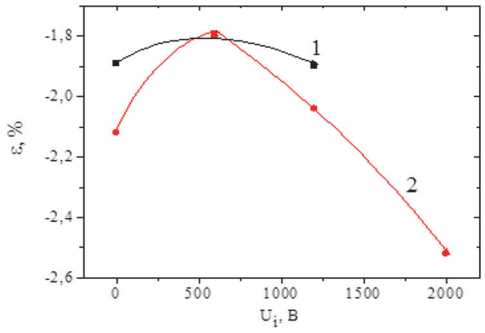

Fig. 4. Dependence of the stress-strain state of TiN coatings (crystallites with texture [111]) on the value of the pulsed bias potential; at a constant potential of −230 V and different pressures p_N: *1* — $2 \cdot 10^{-3}$ Torr; 2 — $5 \cdot 10^{-3}$ Torr.

increase, which is obviously a consequence of increasing the intensity and average energy of ion bombardment during deposition.

That is, when the values of U are more than 1000 V, there is a change in the structural state of the coating; and as the pulsed potential rises, the perfection of the texture [110] increases, accompanied by an increase in implantation-stimulated compressive macrostrains (Fig. 3). The latter corresponds to the action of compressive macrostresses. This texture corresponds to minimal radiation damage to the crystal structure growing during high-energy implantation. The change in the macro-stress-strain state is determined by the displacement of the diffraction peaks at oblique measurements ($\sin^2\psi$-method) (Fig. 4).

It is seen that the use of pulsed action to the value of −600 V significantly reduces the stress-strain state from −2.12 % to −1.8 %, at both pressures of the nitrogen atmosphere; then it reaches an almost constant level, which is a consequence of a more uniform distribution of film-forming particles in the coating under pulsed stimulation during deposition. A further increase in the pulsed potential leads to an increase in strains ε; this is especially noticeable at higher pressures of the nitrogen atmosphere. This is due to the increased effect of the high-voltage pulses, when more nitrogen and titanium atoms enter the lattice of titanium nitride ($5 \cdot 10^{-3}$ Torr). In this case, there is an accumulation of defects in the crystal lattice and the macrostrains reach a maximum value of −2.52 %.

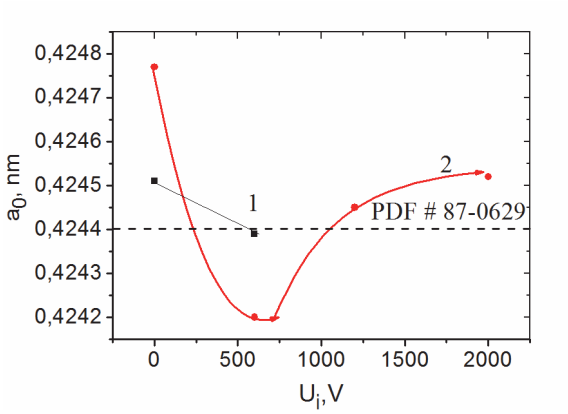

Fig. 5. Dependence of the lattice period on U_i at $U_s = -230$ V and different pressures p_N: *1* — $2 \cdot 10^{-3}$ Torr; *2* — $5 \cdot 10^{-3}$ Torr.

The lattice period a_0 in the unstressed section also changes monotonically without extrema with an increase in the input energy by applying a large U_i (Fig. 5). In this case, with increasing U_i, the lattice period in the unstressed section decreases, which, for the phases including TiN, indicates the appearance of vacancies in the nonmetallic sublattice. The tabular lattice parameter for TiN is $a_0 = 0.4244$ nm (PDF # 87-0629). Thus, an increase in U_i leads to an increase in the lattice period. The latter indicates the appearance of excess (interstitial) atoms in the lattice during deposition.

Measurements by nanoindentation showed the hardness maximum value of 40–42 GPa after action of $U_i = -600$ V with a pulse duration of 10μs. A decrease in hardness to 30–32 GPa at higher U_i can be explained by relaxation processes: a decrease in microstrains and a simultaneous coarsening of crystallites. A similar dependence was observed at the maximum pulse duration (16 μs) for both pressures of the nitrogen atmosphere [27].

4. Conclusions

Using the principles of structural engineering, a coating technology has been developed that makes it possible to influence the texture during the deposition process in a wide range, providing the coating with the required set of functional properties. Computer simulation of the deposition process clearly shows the area of the influence and the number of vacancies created by titanium and nitrogen ions during the deposition of the coating. It is shown that the supply of high-voltage pulsed bias potential increases the mobility of particles and leads

to relaxation processes. The latter provides a reduction in the growth compressive stresses. The reasons of structural changes observed in titanium nitride coatings were analyzed, based on the mechanism of formation of surface layers of vacuum-arc coatings under conditions of implantation processes stimulated by supply of a negative potential to the substrate.

References

1. M.Chernets, M.Pashechko, A.Nevchaz, Doslidzhennya and Rozrakhunok of Tribosystems Kovzannya, Methods of Advancing Durability and Weariness, Kolo, Drogobich, (2001) [in Ukrainian].
2. O.V.Zakalov, I.O.Zakalov, Basics of Rubbing and Business in Cars: Navch. Posibnik, View of TNTU im. I. Pulyuya, Ternopil (2011) [in Ukrainian].
3. V.A.Boguslaev, L.V.Ivshchenko, A.Ya.Kachan, V.F.Mozgovoy, Contact Interaction of GTE Mating Parts, Publishing House of Motor Sich OJSC, Zaporozhye (2009) 328 p.
4. A.V.Chichinadze, E.M.Berliner, E.D.Brown, Friction, Wear and Lubrication. Tribology and Tribology, Mashinostroenie, Moscow (2003) [in Russian].
5. K.A.Krylov, M.E.Khaimnzon, Durability of Aircraft Friction Units, Transport, Moscow (1976) [in Russian].
6. V.A.Trofimov, V.M.Beletskiy, *Technological Systems*, **35**, 56 (2002).
7. A.S.Bychkov, V.M.Fedirko, *Physical Mechanics of Materials*, **1**, 14 (2010).
8. A.S.Bychkov, Problems of Rubbing and Building, **1**, 98 (2016).
9. S.Veprek, M.G.J.Veprek-Heijman, P.Karvankova, J.Prochazka, *Thin Solid Films*, **476**, 1 (2005).
10. O.V.Sobol, *FTT*, **49**, 6 (2007).
11. A.D.Pogrebnyak, A.P.Shpak, N.A.Azarenkov, V.M.Beresnev, *Phys.*, **179**, 35 (2009).
12. A.I.Gusev, Nanomaterials, Nanostructures, Nanotechnology, Fizmalit, Moscow (2005).
13. A.P.Shpak, P.G.Cheremskoy, Yu.aKunitskiy, O.V.Sobol, Cluster and Nanostructured Materials, vol. 3, Academperiodika, Kiev (2005).
14. R.A.Andrievsky, A.V.Ragulya, Nanostructured Materials, Academy, Moscow (2005).
15. Ch.Poole, F.Owens, Nanotechnology, Technosphere, Moscow (2004).
16. Yu.I.Golovin, Introduction to Nanotechnology, Mechanical Engineering, Moscow (2007).
17. N.P.Lyakishev, M.I.Alymov, *Russian Nanotechnology*, **1**, 71 (2006).
18. N.I.Noskov, R.R.Mulyukov, Submicrocrystalline and Nano-crystalline Metals and Alloys, Ural Branch of the Russian Academy of Sciences, Yekaterinburg (2003).
19. O.V.Sobol', A.A.Andreev, V.A.Stolbovoj et al., *VANT*, **4-98/74**, 174 (2011).
20. O.V.Sobol', O.A.Shovkoplyas, *Technical Physics Letters*, **39**, 536 (2013).
21. I.C.Noyanand, J.B.Cohen, Residual Stress Measurement by Diffraction and Interpretation, Springer-Verlag: NewYork (1987).
22. C.Genzel, *Phys. Stat. Sol. (a)*, **159**, 283 (1997).
23. C. Genzel, W.Reinmers, *Phys. Stat. Solidi: A-Applied Research*, **166**, 751 (1998).
24. E.Aznakayev, Micron-Gamma for Estimation the Physico-mechanical Properties of Micromaterials, Proc. of the Intern. Conf. "Small Talk — 2003", San Diego, California, USA (2003), p.8.
25. V.F.Gorban', *Powder Metallurgy and Metal Ceramics*, **47**, 493 (2008).
26. O.V.Sobol, A.A.Andreev, S.N.Grigoriev et al., *Metallofiz.the Latest Technol.*, **35**, 943 (2013).
27. N.V.Pinchuk, O.V.Sobol', V.V.Subbotina, G.I.Zelenskaya, *Functional Materials*, **27**, 595 (2020).